Synthesis, Structures, and C-H Bond Activation Reactions of $HRe(PR_3)_2(L)_3$ Complexes

William D. Jones*† and John A. Maguire

Department of Chemistry, University of Rochester, Rochester, New York 14627

Received October 14, 1986

The reactions of $(\eta^4\text{-}C_5H_6)Re(PPh_3)_2H_3$ with a variety of ligands L are found to give substitution products in which cyclopentene is displaced from the metal. For the cases in which L = CO or CNR (R = Me, Et, *i*-Pr, *t*-Bu, CH_2CMe_3, c-C_6H_{11}, and 2,6-xylyl), products of the formulation $HRe(PPh_3)_2L_3$ are obtained. The complex $HRe(PPh_3)_2(CNMe)_3$ was found to be of the *mer* configuration, crystallizing in the triclinic space group $P\bar{1}$ with a = 11.201 (5) Å, b = 18.630 (6) Å, c = 9.433 (4) Å, α = 98.74 (4)°, β = 105.00 (4)°, γ = 103.05 (4)°, V = 1805.4 (3.3) Å^3, d_{calcd} = 1.536 g/cm^3, and Z = 2. Reaction with L = PMe_3 is found to give only $HRe(PMe_3)_5$, which crystallizes in the monoclinic space group $C2/m$ with a = 15.698 (6) Å, b = 10.869 (5) Å, c = 15.092 (4) Å, β = 107.88 (3)°, V = 2450.5 (3.1) Å^3, d_{calcd} = 1.538 g/cm^3, and Z = 4. This complex undergoes H/D exchange of all hydrogen atoms with C_6D_6 solvent upon irradiation or heating to 105 °C and catalytically exchanges deuterium from the solvent into added free PMe_3. With L = PEt_3, an intermediate in which one of the PPh_3 ligands has undergone ortho metalation is isolated. $H_2Re(PEt_3)_3(PPh_2C_6H_4)$ was found to crystallize in the orthorhombic space group *Pcab* with a = 19.285 (5) Å, b = 32.437 (7) Å, c = 12.150 (4) Å, V = 7600.7 (5.7) Å^3, d_{calcd} = 1.405 g/cm^3, and Z = 8. The complex shows a pentagonal-bipyramid geometry with axial PEt_3 groups. Fluxional interchange of the two distinct hydride ligands and the axial and equatorial PEt_3 ligands is observed. Reaction with L = DMPE gives $ReH(DMPE)_2(PPh_3)$, which was found to crystallize in the triclinic space group $P\bar{1}$ with a = 10.523 (6) Å, b = 18.599 (8) Å, c = 10.511 (5) Å, α = 90.94 (4)°, β = 117.37 (4)°, γ = 105.85 (5)°, V = 1732.9 (8.5) Å^3, d_{calcd} = 1.512 g/cm^3, and Z = 2. The complex displays a cis-octahedral structure.

Introduction

Recently many rhenium hydride complexes have been shown to be capable of activating the C-H bonds of arenes and alkanes. These compounds include $Re(PR_3)_2H_7$,[1-3] $(C_5Me_5)Re(PMe_3)_3$,[4] $CpRe(PMe_3)_3$,[4] $CpRe(PPh_3)_2H_2$,[5] $Re(diphos)_2H_3$,[6] $(C_6H_6)Re(PPh_3)_2H$,[7] and $Re(PR_3)_3H_5$.[6,8] The evidence for C-H activation by these compounds has included H/D exchange, alkane dehydrogenation, and direct observation of the unstable oxidative addition adduct. All of these complexes lack a ligand capable of functionalizing the activated C-H bond, and transformation of the alkane has been limited to catalytic trans-olefination of alkanes and 3,3-dimethyl-2-butene by $Re(PR_3)_2H_7$.[2]

Several of our earlier studies with rhodium[9] and ruthenium[10] have been directed at using isocyanide as a trapping ligand for the C-H oxidative addition adduct. The syntheses of several electron-rich Re(I) complexes of the general formula $HRe(P)_2(L)_3$ (P = PPh_3, PMe_3; L = PMe_3, CO, CNR; R = methyl, ethyl, isopropyl, *tert*-butyl, neopentyl, cyclohexyl, 2,6-xylyl) from the reactive precursor $(\eta^4\text{-}C_5H_6)Re(PPh_3)_2H_3$[11] are presented in this paper. These complexes were prepared in an effort to make new species capable of C-H activation that also possessed a ligand suitable for functionalization of the activated bond. We describe here the catalytic H/D exchange and intramolecular metalation reactions of these complexes.

Results and Discussion

A. Preparation and Structure of $HRe(PPh_3)_2(L)_3$. The synthesis of the class of compounds *trans,mer*-$HRe(PPh_3)_2(L)_3$ begins with a benzene solution of $(\eta^4\text{-}C_5H_6)Re(PPh_3)_2H_3$ (1) in the presence of a 2-electron donor ligand, L. Heating of 1 with excess L at 40-50 °C in all cases results in the hydrogenation of the η^4-cyclopentadiene ring to cyclopentene (eq 1). When L is CO or CNR (R

$$(\eta^4\text{-}C_5H_6)Re(PPh_3)_2H_3 + 3L \rightarrow HRe(PPh_3)_2L_3 + c\text{-}C_5H_8 \quad (1)$$
$$\mathbf{1} \qquad\qquad \mathbf{2a\text{-}g}$$

L = CNMe (**2a**), CNEt (**2b**), $CNCHMe_2$ (**2c**), $CNCMe_3$ (**2d**), $CNCH_2CMe_3$ (**2e**), CN(c-C_6H_{11}) (**2f**), CN(2,6-xyl) (**2g**)

= methyl, ethyl, isopropyl, *tert*-butyl, neopentyl, cyclohexyl, and 2,6-xylyl (xyl)), the organometallic product is the single Re(I) (**2a-g**) isomer resulting from substitution of 3 equiv of L at the metal center for two hydride ligands and the η^4-C_5H_6 ring.

The unequivocal assignment of the isomer was not possible from ^{1}H NMR data, since either isomer A (trans, *mer*) or B (cis, *fac*) would have the same relative ^{1}H NMR spectrum indicative of equivalent phosphines, two kinds of isocyanide ligand in a 2:1 ratio, and a hydride resonance split into a triplet by the equivalent phosphine ligands. A third cis, *mer* isomer (C) would have distinct phosphine and ioscyanide ligands. While the IR spectrum in the C≡N stretching region is theoretically capable of distin-

† A.P. Sloan Fellow, 1984-1986. Camille and Henry Dreyfus Teacher Scholar, 1985-1987.

(1) Chatt, J.; Coffey, R. S. *J. Chem. Soc. A* **1969**, 1963-1972. Chatt, J.; Coffey, R. S. *J. Chem. Soc., Chem. Commun.* **1966**, 545-546.
(2) Baudry, D.; Ephritikhine, M.; Felkin, H. *J. Chem. Soc., Chem. Commun.* **1980**, 1243-1244. Felkin, H.; Fillebeen-Khan, T.; Gault, Y.; Holmes-Smith, R.; Zakrzewski, J. *Tetrahedron Lett.* **1984**, *25*, 1279-1282. Baudry, D.; Ephritikhine, M.; Felkin, H.; Zakrzewski, J. *Tetrahedron Lett.* **1984**, *25*, 1283-1284.
(3) Zeiher, E. H. K.; DeWit, D. G.; Caulton, K. G. *J. Am. Chem. Soc.* **1984**, *106*, 7006-7011.
(4) Bergman, R. G.; Seidler, P. F.; Wenzel, T. T. *J. Am. Chem. Soc.* **1985**, *107*, 4358-4359.
(5) Jones, W. D.; Maguire, J. A. *Organometallics* **1986**, *5*, 590-591.
(6) Roberts, D. A.; Geoffroy, G. L. *J. Organomet. Chem.* **1981**, *214*, 221-231.
(7) Jones, W. D.; Fan, M. *Organometallics* **1986**, *5*, 1057-1059.
(8) Green, M. A.; Huffman, J. C.; Caulton, K. G.; Rybak, W. K.; Ziolkowski, J. J. *J. Organomet. Chem.* **1981**, *218*, C39-C43.
(9) Jones, W. D.; Feher, F. J. *Organometallics* **1983**, *2*, 686-687.
(10) Jones, W. D.; Kosar, W. P. *Organometallics* **1986**, *5*, 1823-1829. Jones, W. D.; Kosar, W. P. *J. Am. Chem. Soc.* **1986**, *108*, 5640-5641.
(11) Jones, W. D.; Maguire, J. A. *Organometallics* **1985**, *4*, 951-953. Jones, W. D.; Maguire, J. A. *Organometallics* **1987**, *6*, 0000.

0276-7333/87/2306-1728$01.50/0

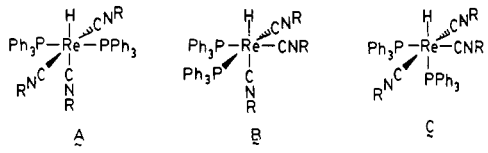

A B C

guishing between molecules with C_{2v} and C_s symmetry, the IR spectrum shows either one or two strong broad bands in the 1900–2000 cm^{-1} region. A single-crystal X-ray diffraction study of the $HRe(PPh_3)_2(CNMe)_3$ complex provided the necessary information for the assignment of the isomer as the *trans,mer*-$HRe(PPh_3)_2(CNMe)_3$ (**2a**), Figure 1.

The structure of $HRe(PPh_3)_2(CNMe)_3$ is best described as a distorted octahedron with the two equatorial isocyanide ligands along with the phosphines bent toward the hydride ligand. The C21–Re–C31 angle is distorted from the ideal of 180° to 164.1°, and the P1–Re–P2 angle is distorted to 175°. Additionally the C–N–C isocyanide angles are significantly bent from their free ligand linearity. The angles for C21–N2–C22 and C31–N3–C32 are 163.2 and 165.0°, respectively, while the C11–N1–C12 angle in the isocyanide which is trans to the pure σ-donating hydride ligand is bent even further from 180° to 153.9°. Both the cis Re–C11–N1 and trans Re–C21–N2 bond angles are 177.4°, whereas the cis Re–C31–N3 is bent slightly to 173.6°. Table I gives distances and angles, and Table II lists fractional atomic coordinates.

The electron-rich Re(I) center apparently donates significant electron density into the C=N π systems which results in a decrease in the C=N bond order and a change in the hybridization at nitrogen from sp toward sp^2, causing the deviation from linearity. This analysis if further supported when the C—N bond lengths are compared. The bond lengths for the equatorial C=N's are 1.160 (11) and 1.161 (11) Å, while the C=N distance for the single isocyanide ligand trans to the hydride is lengthened more to 1.211 (11) Å, indicating a greater weakening of the C=N bond and more donation into the π^* system.

Understanding the mechanism of these syntheses is aided by previously reported spin saturation transfer (SST) experiments that show reversible migration of a hydride ligand to the ring in 1 at temperatures above 40 °C to generate a 16-electron allyl complex (eq 2)[11] and by the

(2)

observation of 1 equiv of cyclopentene as a product during all of these syntheses. The proposed mechanism for the formation of these complexes is shown in Scheme I. Since migration of hydride ligand to the η^4-C_5H_6 ring becomes rapid and reversible at 40 °C, one obvious question is to ask if this step is rate determining in the formation of $HRe(PPh_3)_2(L)_3$ complexes. If this first step is rate-determining, then there should be no dependence on the concentration of the entering ligand L.

Examination of the effect of 2,6-xylyl isocyanide concentration (in excess over 1) on the rate of reaction 1 indicates that the observed pseudo-first-order rate constant k_{obsd} is linearly dependent on [CNR], as shown in Figure 2. The slope of this line according to the rate expression indicated in eq 3 gives a value of k_1k_2/k_{-1} of 1.85×10^{-4}

$$-\frac{d[HRe(PPh_3)_2L_3]}{dt} = \frac{k_1k_2[L]}{k_{-1}}[1] = k_{obsd}[1] \qquad (3)$$

M^{-1} s^{-1}. Since none of the η^3-C_5H_7 intermediate is observed

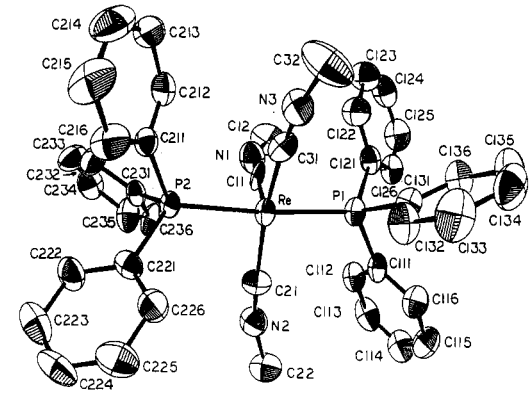

Figure 1. ORTEP drawing of $HRe(PPh_3)_2(CNMe)_3$. Ellipsoids are shown at the 50% probability level. Hydride ligand was not located.

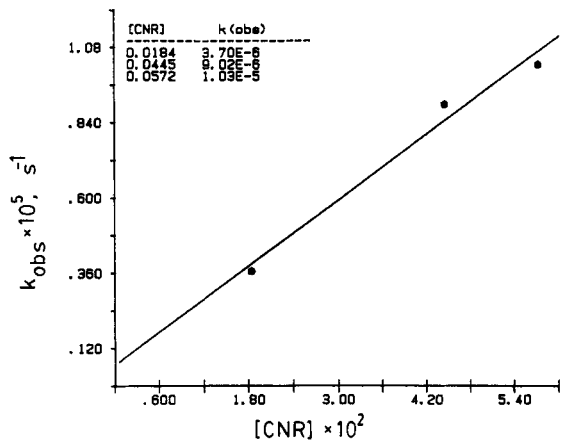

Figure 2. Plot of k_{obsd} vs. [CN-2,6-xylyl] for reaction of 1 with CN-2,6-xylyl isocyanide in benzene at 40 °C.

Table I. Selected Distances (Å) and Angles (deg) for $HRe(PPh_3)_2(CNMe)_3$

	Bond Distances		
Re–P1	2.369 (2)	Re–C31	2.003 (9)
Re–P2	2.383 (2)	N1–C11	1.210 (11)
Re–C11	1.922 (9)	N2–C21	1.168 (11)
Re–C21	1.991 (9)	N3–C31	1.176 (11)
	Bond Angles		
P1–Re–P2	174.99 (7)	C11–Re–C21	96.5 (4)
Re–C11–N1	177.3 (8)	C11–Re–C31	99.0 (4)
Re–C21–N2	177.4 (8)	C21–Re–C31	164.0 (3)
Re–C31–N3	173.6 (8)	P1–Re–C11	87.3 (2)
C11–N1–C12	154 (1)	P1–Re–C21	92.4 (3)
C21–N2–C22	163 (1)	P1–Re–C31	84.3 (3)
C31–N3–C32	166 (1)	P2–Re–C11	91.3 (2)
		P2–Re–C21	92.5 (3)
		P2–Re–C31	91.1 (3)

Scheme I

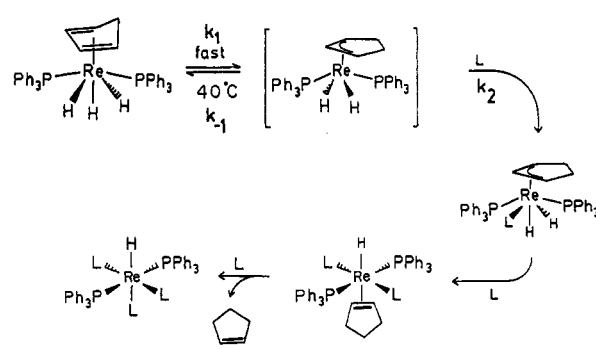

directly, k_1/k_{-1} must be much less than one, indicating that $k_2 > 10^{-2}$ M^{-1} s^{-1}. The rate of hydride to ring migration

Table II. Fractional Atomic Coordinates for $HRe(PPh_3)_2(CNMe)_3$

atom	x	y	z	B, Å²
Re	0.27974 (4)	0.24506 (2)	0.20595 (5)	2.518 (9)
P1	0.3849 (3)	0.1533 (2)	0.1441 (3)	2.79 (6)
P2	0.1850 (3)	0.3444 (2)	0.2584 (3)	2.62 (6)
N1	0.120 (1)	0.2075 (7)	−0.135 (1)	5.4 (3)
N2	0.083 (1)	0.1274 (6)	0.303 (1)	4.5 (3)
N3	0.539 (1)	0.3598 (6)	0.211 (1)	4.7 (3)
C11	0.185 (1)	0.2224 (6)	−0.004 (1)	3.0 (2)
C12	0.083 (2)	0.169 (1)	−0.289 (2)	6.7 (5)
C21	0.153 (1)	0.1716 (7)	0.265 (1)	3.6 (3)
C22	0.026 (1)	0.0627 (8)	0.350 (1)	5.0 (4)
C31	0.439 (1)	0.3192 (6)	0.203 (1)	3.4 (3)
C32	0.671 (1)	0.400 (1)	0.250 (2)	7.4 (5)
C111	0.319 (1)	0.0570 (6)	0.167 (1)	3.2 (3)
C112	0.192 (1)	0.0180 (7)	0.087 (1)	3.9 (3)
C113	0.137 (1)	−0.0538 (7)	0.104 (2)	4.9 (3)
C114	0.207 (1)	−0.0850 (7)	0.206 (2)	5.3 (4)
C115	0.331 (1)	−0.0470 (7)	0.287 (2)	5.4 (4)
C116	0.390 (1)	0.0246 (7)	0.269 (1)	4.2 (3)
C121	0.384 (1)	0.1357 (7)	−0.056 (1)	3.5 (3)
C122	0.422 (1)	0.1980 (7)	−0.113 (1)	4.4 (3)
C123	0.418 (1)	0.1885 (8)	−0.264 (1)	5.2 (4)
C124	0.374 (1)	0.1169 (9)	−0.357 (1)	5.5 (4)
C125	0.340 (1)	0.0556 (8)	−0.300 (1)	5.1 (4)
C126	0.346 (1)	0.0642 (6)	−0.149 (1)	3.8 (3)
C131	0.557 (1)	0.1724 (6)	0.244 (1)	3.2 (3)
C132	0.608 (1)	0.2145 (8)	0.386 (2)	4.9 (4)
C133	0.741 (1)	0.2309 (9)	0.463 (2)	6.3 (4)
C134	0.816 (1)	0.2008 (9)	0.392 (2)	6.4 (4)
C135	0.766 (1)	0.1564 (9)	0.252 (2)	5.8 (4)
C136	0.637 (1)	0.1417 (8)	0.177 (2)	4.7 (3)
C211	0.282 (1)	0.4380 (6)	0.258 (1)	3.1 (3)
C212	0.311 (1)	0.4477 (7)	0.125 (1)	3.9 (3)
C213	0.388 (1)	0.5147 (7)	0.118 (1)	4.7 (3)
C214	0.441 (1)	0.5732 (8)	0.244 (2)	6.0 (4)
C215	0.416 (2)	0.5647 (8)	0.375 (2)	6.2 (4)
C216	0.335 (1)	0.4974 (7)	0.382 (1)	5.1 (4)
C221	0.150 (1)	0.3634 (7)	0.440 (1)	3.4 (3)
C222	0.053 (1)	0.3960 (8)	0.455 (1)	4.5 (3)
C223	0.032 (1)	0.4109 (9)	0.595 (2)	5.9 (4)
C224	0.102 (1)	0.3911 (9)	0.713 (1)	5.7 (4)
C225	0.193 (1)	0.358 (1)	0.696 (1)	6.1 (4)
C226	0.218 (1)	0.3427 (8)	0.558 (1)	4.5 (3)
C231	0.030 (1)	0.3399 (6)	0.124 (1)	3.0 (3)
C232	−0.001 (1)	0.4032 (7)	0.082 (1)	4.3 (3)
C233	−0.119 (1)	0.3971 (8)	−0.014 (2)	5.4 (4)
C234	−0.209 (1)	0.3292 (8)	−0.071 (2)	5.3 (4)
C235	−0.184 (1)	0.2654 (8)	−0.025 (2)	5.3 (4)
C236	−0.062 (1)	0.2715 (7)	0.069 (2)	4.1 (3)

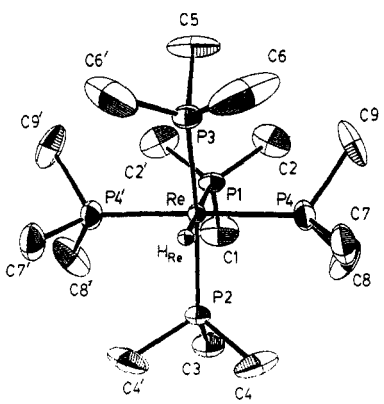

Figure 3. ORTEP drawing of $HRe(PMe_3)_5$. Ellipsoids are shown at the 50% probability level. Hydride ligand was not located but is shown in idealized location.

is ~1 s^{-1} at 40 °C on the basis of the SST results, which represents an upper limit for the rate of reaction of the intermediate with 2,6-xylyl isocyanide. Combining this rate with the concentrations of isocyanide used here, k_2 can be bracketed between 10^{-2} and ~10 M^{-1} s^{-1}. Consequently, hydride migration is rapid and reversible with coordination of L being rate-determining.

Table III. Selected Distances (Å) and Angles (deg) for $HRe(PMe_3)_5$

Bond Distances			
Re–P1	2.372 (2)	Re–P3	2.342 (2)
Re–P2	2.371 (2)	Re–P4	2.369 (2)
Bond Angles			
P1–Re–P2	103.92 (6)	P2–Re–P4	89.38 (2)
P1–Re–P3	101.27 (6)	P3–Re–P4	90.26 (3)
P1–Re–P4	90.85 (2)	P4–Re–P4	178.19 (5)
P2–Re–P3	154.81 (8)		

Table IV. Fractional Atomic Coordinates for $HRe(PMe_3)_5$

atom	x	y	z	B, Å²
Re	0.16992 (1)	0.000	0.23252 (1)	1.366 (9)
P1	0.3169 (1)	0.000	0.3390 (1)	2.45 (4)
P2	0.1929 (1)	0.000	0.0844 (1)	2.27 (4)
P3	0.0833 (1)	0.000	0.3342 (1)	2.56 (4)
P4	0.16820 (7)	−0.2179 (2)	0.23000 (7)	2.97 (5)
C1	0.4155 (5)	0.000	0.2960 (6)	5.4 (2)
C2	0.3552 (4)	−0.1248 (6)	0.4249 (4)	4.9 (2)
C3	0.3047 (5)	0.000	0.0658 (5)	3.9 (2)
C4	0.1406 (4)	−0.1237 (5)	0.0019 (3)	4.4 (1)
C5	0.1290 (6)	0.000	0.4596 (6)	6.3 (3)
C6	0.0023 (4)	−0.1188 (8)	0.3235 (5)	9.8 (2)
C7	0.0698 (4)	−0.2985 (5)	0.1526 (4)	4.1 (1)
C8	0.2593 (4)	−0.2964 (6)	0.1966 (4)	5.8 (2)
C9	0.1796 (5)	−0.3109 (6)	0.3376 (4)	6.0 (2)

B. Preparation and Structure of $HRe(PMe_3)_5$. The thermolysis of **1** at 40 °C in C_6H_6 in the presence of PMe_3 (10 equiv) for 2 days results in the formation of a completely phosphine-substituted complex, $HRe(PMe_3)_5$ (**2h**), in 93% isolated yield.[12] When this reaction was carried out in a sealed NMR tube at 40 °C in C_6D_6 and followed by ^1H NMR spectroscopy, no evidence for the presumed intermediate in the reaction, $HRe(PPh_3)_2(PMe_3)_3$, was observed. At completion ^1H NMR resonances for cyclopentene, free PPh_3, and **2h** integrated to a 1:2:1 mole ratio, respectively (eq 4). The ^1H NMR spectrum of the molecule displayed the expected 4:1 ratio of PMe_3 resonances, but the hydride resonance appeared unexpectedly as a quintet of doublets ($J_{trans} < J_{cis}$) rather than a doublet of quintets ($J_{trans} > J_{cis}$). A structural examination of the molecule was undertaken to determine if any unusual features were present in the molecule.

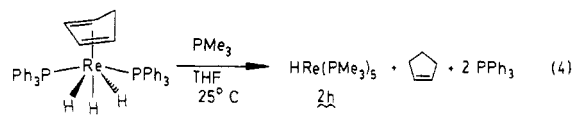

Recrystallization of the crude products from ether afforded large plates. A single-crystal X-ray structure at −41 °C showed the expected octahedral disposition of ligands with two of the trans equatorial phosphines bent toward the hydride ligand, Figure 3. The P2–Re–P3 angle is distorted from the ideal 180 to 154.8°, while the P4–Re–P4′ angle is only slightly distorted to 178.1°. A final peak search following placement of the methyl hydrogens in idealized locations showed a peak near the rhenium in the position close to that expected for the hydride ligand, but not in the ideal octahedral site. The axial HRe–Re–P1 angle is 167.7° rather than the expected 180°, and the

(12) Also prepared in 18% yield. See: (a) Chiu, K. W.; Howard, C. G.; Rzepa, H. S.; Sheppard, R. N.; Wilkinson, G.; Galas, A. M.; Hursthouse, M. B. *Polyhedron* **1982**, *1*, 441–451. (b) Gibson, V. C.; Graimann, C. E.; Hare, P. M.; Green, M. L. H.; Bandy, J. A.; Brebenik, P. D.; Prout, K. *J. Chem. Soc., Dalton Trans.* **1985**, 2025–2035.

Re–H distance was only 1.21 Å as opposed to the expected 1.6 Å. The off-center position of the hydride peak is believed to be an artifact of the structural solution rather than having any real structural significance. The Re–P distances fall in the range 2.34–2.37 Å. Table III gives distances and angles, and Table IV lists fractional atomic coordinates.

The reaction sequence employed in the preparation of **2h** is similar to that previously reported by Felkin for the reaction of $P(OMe)_3$ with $Re(PPh_3)_2(diene)H_3$ complexes.[2] These reactions led to the formation of 1-alkene and $HRe[P(OMe)_3]_5$,[2] products similar to the presently observed cyclopentene and $HRe(PMe_3)_5$. Other metal complexes such as $HRuCl(PPh_3)_3$[13] are known that hydrogenate dienes to olefins, and others such as $[Ir(COD)(PPh_3)_2]^+$[14] hydrogenate cyclooctadiene to cyclooctene.

C. C–H Bond Activation by $HRe(PMe_3)_5$. The electron-rich complex $HRe(PMe_3)_5$ has been found to undergo rapid intramolecular H/D exchange in the presence of C_6D_6 solvent at 105 °C and during irradiation (200-W Hg, 365-nm band-pass filter). In an experiment to determine the lability of the PMe_3 ligand, ^1H NMR analysis of a C_6D_6 solution containing $HRe(PMe_3)_5$ (3 mg, 13 mmol) and $P(CD_3)_3$ (10 equiv) began to show the resonance for free PMe_3 at 75 °C. At 105 °C equilibrium was reached between coordinated and free phosphine in less than 15 min (eq 5). Integration of the free PMe_3 reso-

$$HRe(PMe_3)_5 + P(CD_3)_3 \rightleftharpoons HRe(PMe_3)_{5-x}[P(CD_3)_3]_x + PMe_3 \quad (5)$$

nance relative to the coordinated PMe_3 resonances (standardized to a small amount of silicone grease present in the sample) showed 71% exchange (ideal predicted with 10 equiv of $P(CD_3)_3$ would be 67%) after 15 min. The hydride resonance is only slightly exchanged (5–10%) during this time. Even this small amount of H/D exchange is surprising in the presence of 10 equiv of phosphine.

Thermolysis of pure **2h** in C_6D_6 solvent at 105 °C for 21 min results in nearly complete exchange (90%) of all protons for deuterium. This result was verified by ^2H NMR integration against C_6D_{12} internal standard. Deuterium NMR analysis of the solution showed broadened singlets at δ 1.454 and 1.351. The broadening is due to unresolved splitting of the deuterium resonance by as yet unexchanged hydrogen left in the molecule. Integration of these resonances is about 4:1, which would be expected for the four equatorial phosphines relative to the single axial phosphine. After 30 min of thermolysis no signal is observed for the molecule in a ^1H NMR spectrum of the sample. A ^2H NMR spectrum now shows two sharpened resonances for the fully deuteriated coordinated phosphine ligands.

In an analogous experiment, irradiation of a sealed NMR tube containing a C_6D_6 (0.4 mL) solution of **2h** (3 mg) and $P(CD_3)_3$ (10 equiv) showed that equilibrium between free and coordinated phosphine was reached after only 4 min. A ^1H NMR spectrum after 8 min irradiation time of a solution containing only **2h** (3 mg) in C_6D_6 (0.4 mL) with c-C_6D_{12} (2 equiv) showed 80% exchange of deuterium into the complex by comparison to an integration standard (silicone grease). After 30 min of irradiation, no signal for **2h** was observed in the ^1H NMR spectrum. Integration of the ^2H NMR signal vs. added c-C_6D_{12} (2 equiv) confirmed the nearly quantitative presence of the deuteriated complex. Gradual yellowing of the solution was observed during irradiation. After 1 h of irradiation time, the slow degradation of the complex was confirmed by the presence of a resonance (δ 0.74) for a small amount of free $P(CD_3)_3$ (5%) in the ^2H NMR.

In an experiment to determine the usefulness of **2h** as a catalyst for deuteriation of PMe_3, a solution of **2h** (3 mg, 0.0053 mmol) and PMe_3 (10 equiv) in C_6D_6 (0.4 mL) was heated to 105 °C. After 24 h ^1H NMR integration of coordinated and free phosphine vs. silicone grease standard showed only 15% residual proton resonances compared with those before thermolysis. ^2H NMR integration confirmed this result. No $P(CH_3)_3$ resonance was observed after 48 h at 105 °C, and ^2H NMR integration of the free and coordinated phosphine resonance showed the expected 2:1 ratio between free and coordinated $P(CD_3)_3$.

An attempt to employ D_2 gas as the deuterium source was investigated by irradiating **2h** in C_6H_6 solvent. No deuterium incorporation into **2h** was observed. The lack of H/D exchange is attributed to the formation of a stable tetrakis(phosphine)trihydride complex and was verified by monitoring the irradiation of **2h** in C_6D_6 solvent under an atmosphere of H_2. A new product assigned as $ReH_3(PMe_3)_4$ is observed with a hydride resonance at δ –8.129 (quint, J = 20.2 Hz, 3 H) and a PMe_3 resonance at 1.524 (s, 36 H).[15]

Neither thermolysis (105 °C) nor photolysis (200-W Hg, 365-nm band-pass filter) of a solution of $HRe(PMe_3)_5$ (3 mg, 0.0053 mmol) in C_6D_6/C_3H_8 (3:1, v/v) resulted in catalytic H/D exchange between the solvents, and in similar experiments no exchange of deuterium into $HRe(PMe_3)_5$ was observed during thermolysis or photolysis in THF-d_8. However, a ^1H NMR spectrum recorded at –70 °C after photolysis of a $HRe(PMe_3)_5$ solution in THF-d_8 at –55 °C shows several new hydride resonances as well as a resonance for free PMe_3 (δ 0.945) and two broad resonances at δ 1.614 and 1.298 for new phosphine complexes. The P–H couplings of the new hydride resonances suggest the formulation of the intermediates $HRe(PMe_3)_4L$ (quintet at δ –8.755 (J = 21.1 Hz)), $HRe(PMe_3)_3L_2$ (doublet of triplets at δ –6.354 (J = 56.7, 15.3 Hz)), and $HRe(PMe_3)_2L_3$ (triplet at δ –7.080 (J = 24.7 Hz)) where L = THF-d_8 (eq 6). Further evidence for the formulation of

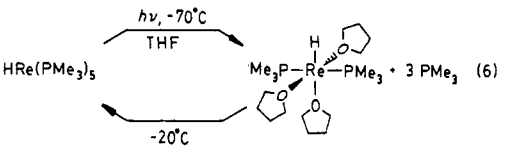

(6)

these very unstable complexes as THF adducts comes from the observation of their rapid and complete disappearance at –20 °C. All of the free PMe_3 recoordinates to regenerate quantitatively the original $HRe(PMe_3)_5$ compound. A ^1H NMR spectrum taken at 25 °C after the low-temperature experiment revealed only resonances for the starting $HRe(PMe_3)_5$ complex with no trace of free PMe_3.

Both aryl and benzyl C–H activation were observed at 105 °C in a solution of $HRe(PMe_3)_5$ (3 mg, 0.0053 mmol) in $C_6D_6/C_6H_5CH_3$ (1:12, v/v) containing c-C_6D_{12} (2 equiv). After 1 week, integration of the new ^2H NMR resonance at δ 2.04 against c-C_6D_{12} showed benzylic activation of 6.6 turnovers and calculation of the aromatic activation indicates a total of 1.7×10^4 turnovers of deuterium in the meta and para positions of the toluene. It is improbable

(13) Birch, A. J.; Williamson, D. H. *Org. React. (N.Y.)* **1976**, *24*, 1–185.
(14) Crabtree, R. H.; Felkin, H.; Khan, T.; Morris, G. E. *J. Organomet. Chem.* **1978**, *144*, C15–C17.

(15) Other ReH_3P_4 complexes are known. See: (a) Ginsberg, A. P.; Tully, M. E. *J. Am. Chem. Soc.* **1973**, *95*, 4749–4751. (b) Freni, M.; Demichelis, R.; Giusto, D. *J. Inorg. Nucl. Chem.* **1967**, *29*, 1433–1439. (c) Bradley, M. G.; Roberts, D. A.; Geoffroy, G. L. *J. Am. Chem. Soc.* **1981**, *103*, 379–384.

that ortho activation has been achieved, although due to the large residual C_6D_6 peak which still dominates the phenyl region, the ortho toluene resonance is not clearly observable.

D. Preparation, Structure, and Dynamic Behavior of $H_2Re(PEt_3)_3(PPh_2C_6H_4)$. In an attempt to make the $HRe(PEt_3)_5$ analogue of $HRe(PMe_3)_5$, $(\eta^4\text{-}C_5H_6)Re(PPh_3)_2H_3$ was reacted for 6 h in C_6H_6 with PEt_3 (10 equiv) at 45 °C. Instead of the expected $HRe(PEt_3)_5$ complex, the product of reaction was the cyclometalated species $H_2Re(PEt_3)_3(PPh_2C_6H_4)$ (eq 7). This complex is fluxional

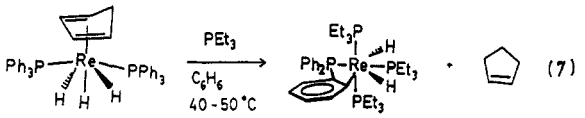

on the ^1H NMR time scale at room temperature, with its hydride resonances at the coalescence limit. The two distinct resonances for the methylene and methyl protons (area 2:3, respectively) of the three PEt_3 ligands are in a 2:1 ratio, indicating two equivalent PEt_3 ligands and a third distinct phosphine ligand. The two resonances in the ortho phenyl region (δ 7.2–7.8) integrate to a ratio 4:1. This is what would be expected for four equivalent ortho protons on two phenyl rings not coordinated to the metal and the one distinct ortho proton remaining on the metalated ring. No other protons on the metalated ring are clearly observable due to the residual C_6D_5H resonance and the meta and para resonances for the unmetalated phenyl protons. Changing solvent from C_6D_6 to THF-d_8 resolves all aromatic resonances for the coordinated ring.

Dynamic ^1H NMR studies of this molecule in toluene-d_8 indicate that at −10 °C the fluxionality of the hydride ligands is frozen out to yield two broad resonances at δ −4.897 and −8.303. However, even at −80 °C the coupling of these hydrides to the phosphines or to each other is not resolved. At temperatures above 40 °C the two distinct kinds of PEt_3 ligands equilibrate to give a single pair of resonances for the equivalent methylene and the methyl protons at δ 1.473 and 0.852, respectively. Spin saturation transfer experiments show magnetization transfer between the hydride ligands as low as −20 °C, but no transfer is observed between the hydrides and the distinct ortho phenyl proton on the metalated ring or between the ortho phenyl protons and the distinct ortho proton on the metalated ring at temperatures up to 85 °C, where the molecule begins to decompose. The exchange rate of the hydrides is calculated to be 3404 s^{-1} at the coalescence temperature (28 °C), yielding a value for $\Delta G^{\ddagger} = 12.7 \pm 0.2$ kcal/mol.[16]

The intramolecular exchange of the PEt_3 ligands is a slower, higher energy process. The calculated rate of exchange at the coalescence temperature (38 °C) of the triethylphosphines is 168 s^{-1} which gives an activation barrier of $\Delta G^{\ddagger} = 15.1 \pm 0.2$ kcal/mol. The mechanisms for these two rapid exchanges are not clear since rapid (>1 s^{-1}) reductive elimination and oxidative addition of the metalated ring was ruled out when spin saturation transfer was not observed between the hydrides and the ortho phenyl protons. In addition, the complex does not react with added PEt_3 at 80 °C to yield $HRe(PEt_3)_5$ and only slowly reacts with H_2 at 80 °C, apparently via loss of PEt_3, to give the ortho-metalated complex $H_4Re(PEt_3)_2(PPh_2C_6H_4)$. In addition, at 80 °C the reaction of $H_2Re(PEt_3)_3(PPh_2C_6H_4)$ with PMe_3 results in substitution of the two axial PEt_3 ligands with PMe_3 to yield $H_2Re(PMe_3)_2(PEt_3)(PPh_2C_6H_4)$ while none of the equatorial ligand is exchanged over 1 h (eq 8). Although the exact

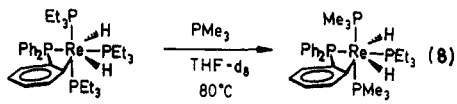

nature of the exchange processes are not understood, the fluxionality of $H_2Re(PEt_3)_3(PPh_2C_6H_4)$ is not surprising since seven-coordinate complexes are well-known to undergo rapid intramolecular ligand exchange processes even under mild conditions.[17]

An X-ray structural determination was successfully undertaken with the hydride ligands being located and refined. Figure 4 reveals a distorted pentagonal-bipyramidal geometry for this complex. The axial PEt_3 ligands are distorted from the ideal 180° to 166.2°, while the 148.9° angle between the two hydride ligands located in the equatorial plane is bisected by the third PEt_3 ligand. The remaining equatorial ligands are the triphenylphosphine

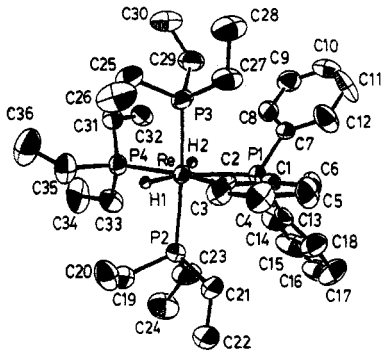

Figure 4. ORTEP drawing of $H_2Re(PEt_3)_3(PPh_2C_6H_4)$. Ellipsoids are shown at the 50% probability level. Hydride ligands were located and refined.

Table V. Selected Distances (Å) and Angles (deg) for $H_2Re(PEt_3)_3(PPh_2C_6H_4)$

	Bond Distances		
Re–H1	1.54 (8)	P1–C1	1.782 (9)
Re–H2	1.40 (8)	C1–C2	1.424 (12)
Re–P1	2.394 (2)	C1–C6	1.384 (12)
Re–P2	2.394 (2)	C2–C3	1.401 (12)
Re–P3	2.400 (3)	C3–C4	1.387 (12)
Re–P4	2.404 (3)	C4–C5	1.371 (13)
Re–C2	2.170 (9)	C5–C6	1.391 (13)
	Bond Angles		
P1–Re–P2	93.46 (8)	Re–P1–C1	88.5 (4)
P1–Re–P3	93.41 (9)	Re–P1–C7	123.9 (3)
P1–Re–P4	138.66 (9)	Re–P1–C13	125.5 (3)
P2–Re–P3	166.16 (9)	P1–C1–C2	98.6 (7)
P2–Re–P4	91.54 (9)	C1–C2–Re	108.3 (7)
P3–Re–P4	91.22 (9)	C1–C2–C3	116.1 (8)
H1–Re–P4	77 (3)	C2–C1–C6	123.0 (9)
H2–Re–P4	72 (3)	C2–C3–C4	120.6 (9)
P1–Re–C2	64.5 (3)	C3–C4–C5	122 (1)
H1–Re–C2	80 (3)	C4–C5–C6	119.9 (9)
H2–Re–P1	67 (3)	C5–C6–C1	118 (1)

(16) $k = \pi\Delta\nu/(2)^{1/2}$, and $\Delta G^{\ddagger}$ is from the Eyring equation.

(17) (a) For other articles that propose reversible chelate dissocation, see: Jones, W. D.; Libertini, E. *Inorg. Chem.* **1986**, *25*, 1794–1800. Dobson, G. R.; Binzet, N. S. *J. Coord. Chem.* **1984**, *13*, 153–157. Dobson, G. R.; Mansour, S. E.; Halverson, D. E.; Erikson, E. S. *J. Am. Chem. Soc.* **1983**, *105*, 5505–5506. Dobson, G. R.; Dobson, C. B.; Halverson, D. E.; Mansour, S. E. *J. Organomet. Chem.* **1983**, *253*, C27–C32. (b) Muetterties, E. L. *Acc. Chem. Res.* **1970**, *3*, 266–274.

Table VI. Fractional Atomic Coordinates for $H_2Re(PEt_3)_3(PPh_2C_6H_4)$

atom	x	y	z	B, Å²
Re	−0.00154 (2)	0.13558 (1)	0.13949 (3)	2.550 (8)
P1	−0.0671 (1)	0.07989 (8)	0.2162 (2)	2.78 (6)
P2	−0.1016 (1)	0.16788 (9)	0.0609 (2)	3.16 (6)
P3	0.1009 (1)	0.11860 (9)	0.2420 (2)	3.45 (7)
P4	0.0661 (2)	0.14989 (9)	−0.0222 (2)	3.25 (6)
C1	−0.0820 (5)	0.1110 (3)	0.3349 (7)	2.9 (2)
C2	−0.0471 (4)	0.1473 (3)	0.2998 (7)	2.8 (2)
C3	−0.0489 (5)	0.1808 (3)	0.3727 (8)	3.8 (3)
C4	−0.0812 (5)	0.1772 (3)	0.4743 (8)	4.2 (3)
C5	−0.1122 (6)	0.1412 (3)	0.5073 (8)	4.5 (3)
C6	−0.1134 (5)	0.1074 (3)	0.4369 (9)	4.3 (3)
C7	−0.0302 (5)	0.0303 (3)	0.2531 (8)	3.0 (2)
C8	0.0127 (5)	0.0088 (3)	0.1806 (9)	4.0 (3)
C9	0.0398 (5)	−0.0296 (3)	0.2070 (9)	4.7 (3)
C10	0.0246 (5)	−0.0481 (3)	0.304 (1)	5.1 (3)
C11	−0.0177 (7)	−0.0289 (4)	0.3753 (9)	6.9 (4)
C12	−0.0461 (7)	0.0104 (4)	0.3498 (9)	6.0 (3)
C13	−0.1506 (5)	0.0605 (3)	0.1630 (8)	3.2 (2)
C14	−0.1534 (6)	0.0398 (3)	0.0671 (9)	5.0 (3)
C15	−0.2147 (7)	0.0241 (4)	0.026 (1)	7.4 (4)
C16	−0.2744 (6)	0.0294 (4)	0.083 (1)	8.9 (4)
C17	−0.2735 (5)	0.0487 (5)	0.178 (1)	8.1 (4)
C18	−0.2126 (5)	0.0664 (4)	0.221 (1)	6.0 (3)
C19	−0.0895 (5)	0.2191 (3)	0.0024 (9)	4.2 (3)
C20	−0.0687 (6)	0.2515 (3)	0.08383 (9)	5.5 (3)
C21	−0.1731 (5)	0.1792 (4)	0.1557 (9)	4.6 (3)
C22	−0.2348 (6)	0.2040 (4)	0.1146 (9)	6.0 (3)
C23	−0.1490 (5)	0.1398 (4)	−0.051 (1)	5.8 (3)
C24	−0.1791 (7)	0.1615 (5)	−0.145 (1)	7.9 (4)
C25	0.1692 (5)	0.1590 (4)	0.243 (1)	5.4 (3)
C26	0.1479 (6)	0.1988 (4)	0.299 (1)	6.9 (4)
C27	0.0887 (6)	0.1089 (4)	0.3896 (8)	5.3 (3)
C28	0.1515 (6)	0.0988 (5)	0.4602 (9)	6.9 (4)
C29	0.1515 (5)	0.0713 (4)	0.2067 (9)	4.8 (3)
C30	0.2294 (6)	0.0714 (4)	0.210 (1)	6.4 (3)
C31	0.1414 (5)	0.1170 (3)	−0.0530 (9)	4.4 (3)
C32	0.1232 (5)	0.0726 (3)	−0.0865 (9)	4.5 (3)
C33	0.0213 (6)	0.1457 (3)	−0.1552 (9)	4.5 (3)
C34	0.0600 (7)	0.1511 (4)	−0.2618 (8)	7.3 (4)
C35	0.1039 (6)	0.2027 (3)	−0.0286 (9)	5.1 (3)
C36	0.1681 (7)	0.2125 (4)	−0.087 (1)	8.7 (4)
H1	0.482 (4)	0.181 (3)	0.654 (7)	5.0
H2	0.495 (4)	0.099 (3)	0.580 (7)	5.0

ligand and its metalated ortho phenyl carbon atom. Bond distances and angles are given in Table V and fractional atomic coordinates listed in Table VI.

E. Preparation, Isomerization, and Structure of $HRe(PPh_3)(DMPE)_2$. Thermolysis of $(\eta^4\text{-}C_5H_6)Re(PPh_3)_2H_3$ and DMPE (5 equiv) in C_6D_6 at 50 °C for 2 weeks results in the formation of two new complexes. These rapidly equilibrating isomers have the stoichiometry $HRe(DMPE)_2(PPh_3)$ (eq 9). ^1H NMR resonances ob-

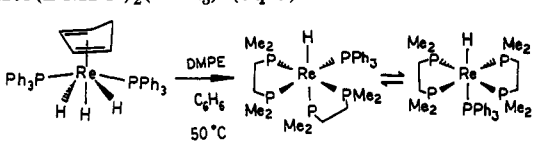

(9)

served for these complexes are consistent with the stereochemical assignment of one isomer as having two equatorial DMPE ligands and PPh_3 trans to hydride while the second isomer has one end of a DMPE and the PPh_3 ligand interchanged resulting in PPh_3 cis to the hydride ligand.

The geometrical configuration of the latter isomer was confirmed by X-ray crystallography, as shown in Figure 5. The molecule displays the cis-octahedral geometry with H–Re–P angles of 73.1°, 98.0°, 78.1°, 88.0° (cis), and 179.0° (trans). The PPh_3 and the end of the DMPE ligand trans to PPh_3 are bent substantially toward the hydride ligand, a distortion seen also in the structures of $HRe(PMe_3)_5$ and

Table VII. Selected Distances (Å) and Angles (deg) for *cis*-$HRe(PPh_3)(DMPE)_2$

Bond Distances			
Re–P1	2.356 (1)	Re–P4	2.356 (1)
Re–P2	2.358 (1)	Re–P5	2.352 (1)
Re–P3	2.349 (1)	Re–HRe	1.66 (3)
Bond Angles			
P1–Re–P2	93.68 (3)	P2–Re–HRe	98 (1)
P1–Re–P3	151.78 (3)	P3–Re–P4	81.32 (3)
P1–Re–P4	97.15 (3)	P3–Re–P5	101.33 (4)
P1–Re–P5	106.88 (3)	P3–Re–HRe	78 (1)
P1–Re–HRe	73 (1)	P4–Re–P5	91.52 (4)
P2–Fe–P3	90.69 (4)	P4–Re–HRe	88 (1)
P2–Re–P4	168.68 (3)	P5–Re–HRe	179 (1)
P2–Re–P5	82.14 (4)		

Table VIII. Fractional Atomic Coordinates for *cis*-$HRe(PPh_3)(DMPE)_2$

atom	x	y	z	B, Å²
Re	0.26500 (1)	0.24541 (1)	0.09385 (1)	1.960 (3)
P1	0.22354 (8)	0.28131 (5)	0.28405 (8)	2.09 (2)
P2	0.00631 (9)	0.18559 (6)	−0.06713 (9)	2.79 (2)
P3	0.32896 (9)	0.16418 (5)	−0.02356 (9)	3.07 (2)
P4	0.52820 (9)	0.30460 (5)	0.21288 (9)	2.85 (2)
P5	0.22658 (9)	0.33722 (5)	−0.05912 (9)	3.11 (2)
C1	0.3908 (3)	0.3134 (2)	0.4670 (3)	2.41 (7)
C2	0.4826 (4)	0.3884 (2)	0.5078 (4)	3.24 (9)
C3	0.6112 (4)	0.4143 (2)	0.6404 (4)	4.2 (1)
C4	0.6527 (4)	0.3643 (3)	0.7356 (4)	4.7 (1)
C5	0.5650 (4)	0.2900 (3)	0.6976 (4)	4.3 (1)
C6	0.4347 (4)	0.2642 (2)	0.5648 (3)	3.28 (9)
C7	0.0997 (3)	0.2037 (2)	0.3277 (3)	2.36 (7)
C8	0.1112 (4)	0.1311 (2)	0.3236 (3)	3.23 (9)
C9	0.0251 (4)	0.0729 (2)	0.3585 (4)	4.0 (1)
C10	−0.0793 (4)	0.0846 (2)	0.3932 (4)	4.1 (1)
C11	−0.0941 (4)	0.1555 (2)	0.3958 (4)	3.82 (9)
C12	−0.0060 (3)	0.2142 (2)	0.3645 (3)	3.16 (8)
C13	0.1414 (3)	0.3575 (2)	0.2914 (3)	2.35 (7)
C14	0.0516 (3)	0.3785 (2)	0.1637 (3)	2.90 (8)
C15	−0.0114 (4)	0.4352 (2)	0.1637 (4)	3.54 (9)
C16	0.0115 (4)	0.4700 (2)	0.2909 (4)	3.60 (9)
C17	0.0979 (4)	0.4494 (2)	0.4206 (4)	3.63 (9)
C18	0.1626 (3)	0.3937 (2)	0.4207 (3)	3.04 (8)
C19	−0.1461 (4)	0.1814 (3)	−0.0248 (4)	4.4 (1)
C20	−0.0703 (5)	0.0868 (3)	−0.1583 (5)	5.6 (1)
C21	−0.0527 (4)	0.2308 (3)	−0.2320 (4)	5.2 (1)
C22	0.2718 (4)	0.1518 (2)	−0.2182 (4)	4.5 (1)
C23	0.2872 (4)	0.0644 (2)	−0.0024 (4)	4.9 (1)
C24	0.5355 (4)	0.1891 (2)	0.0552 (4)	4.4 (1)
C25	0.6551 (4)	0.2849 (2)	0.3900 (4)	4.2 (1)
C26	0.6183 (4)	0.4069 (3)	0.2428 (4)	4.6 (1)
C27	0.6075 (4)	0.2734 (3)	0.1046 (4)	4.3 (1)
C28	0.3113 (5)	0.3538 (3)	−0.1794 (4)	5.5 (1)
C29	0.2701 (4)	0.4385 (2)	0.0049 (4)	4.5 (1)
C30	0.0259 (5)	0.3150 (3)	−0.1977 (4)	5.1 (1)
C101	0.5340 (5)	0.0194 (4)	0.3928 (5)	7.3 (2)
C102	0.4443 (5)	0.0447 (3)	0.5498 (6)	7.3 (2)
C103	0.4788 (5)	0.0629 (3)	0.4425 (6)	7.3 (2)
HRe	0.294 (3)	0.181 (2)	0.202 (3)	2.6 (7)

$HRe(PPh_3)_2(CNMe)_3$, with a P1–Re–P3 bond angle of 151.8°. Distances and angles are given in Table VII and fractional atomic coordinates in Table VIII.

The equilibrium ratio of *trans*-$HRe(DMPE)_2(PPh_3)$ (PPh_3 trans to hydride) to *cis*-$HRe(DMPE)_2(PPh_3)$ (PPh_3 cis to hydride) is 1.56:1 (K_{eq} = 1.56). This ratio gives a calculated $\Delta G°$ = −0.21 kcal/mole at 27 °C between *trans*-$HRe(DMPE)_2(PPh_3)$ and *cis*-$HRe(DMPE)_2(PPh_3)$. *cis*-$HRe(DMPE)_2(PPh_3)$ has been isolated in pure crystalline form as a result of a fortuitous difference in solubility in C_6D_6 between the isomers. Upon standing at room temperature, *cis*-$HRe(DMPE)_2(PPh_3)$ crystallized from the benzene solution. The crystallization of *cis*-$HRe(DMPE)_2(PPh_3)$ drove the equilibrium nearly completely to the left (eq 10) as the benzene solvent was allowed to

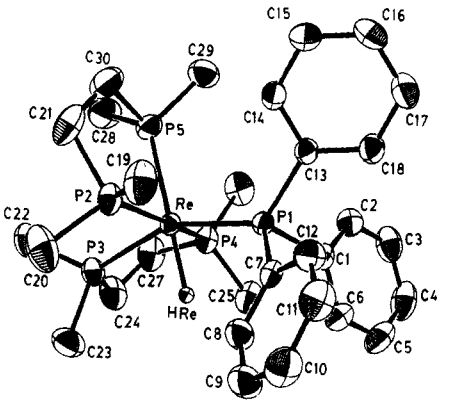

Figure 5. ORTEP drawing of *cis*-HRe(PPh_3)(DMPE)$_2$. Ellipsoids are shown at the 50% probability level. Hydride ligand was located and refined.

slowly evaporate. The ^1H NMR (THF-d_8) of *cis*-HRe(DMPE)$_2$(PPh_3) exhibits eight different resonances for the eight inequivalent methyl groups on the two DMPE ligands (δ 1.777 (d, J = 7.7 Hz, 3 H), 1.480 (d, J = 5.0 Hz, 3 H), 1.433 (d, J = 5.4 Hz, 3 H), 1.307 (d, J = 5.5 Hz, 3 H), 1.255 (d, J = 4.9 Hz, 3 H), 1.171 (d, J = 5.2 Hz, 3 H), 0.544 (d, J = 4.8 Hz, 3 H), 0.266 (d, J = 5.8 Hz, 3 H)) and a hydride resonance (δ −8.381 (m, 1 H)) with complex unresolved splitting. The distinct ortho phenyl proton resonance and the overlapping meta and para resonances are at δ 7.607 (t, J = 7.4 Hz, 6 H) and 7.096 (m, 9 H), respectively.

The thermodynamic isomer *trans*-HRe(DMPE)$_2$(PPh_3) has not been isolated, but the methyl region of the ^1H NMR spectrum for this isomer is the expected much simpler pair of singlets for the two sets (four methyls each) of DMPE methyl protons (δ 1.535 (s, 12 H), 1.125 (s, 12 H)). The hydride resonance assigned to this complex is a quintet of doublets δ −8.772 (J = 24.7, 16.0 Hz) which integrates to one proton. The ortho phenyl resonance is at δ 7.430 (t, J = 8.0 Hz, 6 H), and the meta and para phenyl resonances are at δ 7.034 (m, 9 H). The DMPE methylene proton resonances are obscured by the methyl resonances of both isomers in these complexes.

The mechanism of the interchange between these two isomers has been studied. Pure *cis*-HRe(DMPE)$_2$(PPh_3) was dissolved with PPh_3-d_{15} (5 equiv) in THF-d_8, and the isomerization to an equilibrium mixture of the isomers was monitored by ^1H NMR spectroscopy. Equilibrium between *cis*-HRe(DMPE)$_2$(PPh_3) and *trans*-HRe(DMPE)$_2$(PPh_3) was reached after only 15 min. Even after an additional 1 h at 27 °C no resonances for free PPh_3 (as would be expected if PPh_3 were coming off in the presence of a large excess of PPh_3-d_{15}) were observed in the ^1H NMR spectrum. This observation eliminates the possibility that isomerization proceeds via loss of the PPh_3 ligand from *cis*-HRe(DMPE)$_2$(PPh_3) followed by rearrangement of the coordinatively unsaturated species and readdition of PPh_3 trans to hydride to produce *trans*-HRe(DMPE)$_2$(PPh_3). Instead we believe that isomerization is unimolecular and that it is probable that the reversible loss of one end of a DMPE ligand from *cis*-HRe(DMPE)$_2$(PPh_3) generates the coordinative unsaturation necessary to effect the ligand rearrangement, as indicated in eq 10.[17a] Unimolecular isomerization might also occur by a twist mechanism similar to that for $H_2Fe[P(OMe)_3]_4$ and related molecules.[17b]

The reversible interconversion of the isomers was demonstrated by examining the equilibrium ratios of the complexes at temperatures between −10 and 58 °C by ^1H NMR in THF-d_8. At −10 °C, K_{eq} = 1.67; at 27 °C, K_{eq} = 1.56; and at 58 °C, K_{eq} = 1.41. A plot of ln K_{eq} vs. $1/T$

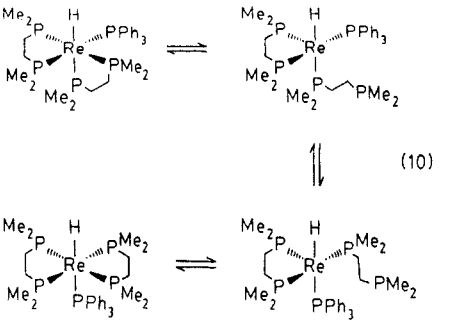

gives values of $\Delta H°$ = −0.42 kcal/mol and $\Delta S°$ = −0.6 eu.

Conclusions

The reactive precursor (η^4-C_5H_6)$ReH_3(PPh_3)_2$ has been shown to be useful for the preparation of a variety of new $HRe(PPh_3)_2L_3$ complexes, as well as $HRe(PMe_3)_5$. In general, the η^4-C_5H_6 complex reacts to give meridionally substituted bis(triphenylphosphine) hydride complexes with the extrusion of cyclopentene. The species HRe(PMe_3)$_5$ is found to reversibly activate both benzene and PMe_3 C–H bonds, resulting in the catalytic deuteriation of PMe_3 using C_6D_6. There is no evidence for the presence of intermediate alkyl or aryl rhenium complexes.

Experimental Section

General Data. Solvents used in glovebox reactions were dried by using potassium or sodium benzophenone and distilled from purple ketyl solution under nitrogen. The solvents used in reactions carried out on the vacuum line or in sealed tubes were distilled by vacuum transfer unless otherwise specified. All filtrations of crude products and recrystallizations were performed under nitrogen atmosphere in a Vacuum Atmospheres Dry-Lab glovebox. Infrared spectra were recorded by using a Mattson Sirius FT infrared spectrometer, and electronic spectra were carried out on a Perkin-Elmer UV–vis spectrophotometer. Proton NMR spectra were recorded by using a Bruker WH-400 NMR spectrometer. Elemental analyses were carried out either at Kodak Instrumental Support Facilities or at Mic-Anal Laboratories.

Rhenium metal (99%) was purchased from Strem Chemicals. Isocyanides were purchased where possible. Synthesis of those not commercially available followed the literature procedure of Ugi.[18] The synthesis of **1** was as previously reported.[11]

Preparation of $HRe(PPh_3)_2L_3$ Complexes from 1. HRe(PPh_3)$_2$(CNMe)$_3$. Complex **1** (50 mg, 0.064 mmol) was sealed in a glass tube with CNMe (26 mg, 0.64 mmol) and C_6H_6 (1 mL). After thermolysis at 50 °C for 6 h yellow crystals formed that were collected, washed with hexanes, and dried under vacuum (49 mg, 91%): ^1H NMR (C_6D_6) δ 8.094 (m, 12 H), 7.125 (7, 12 H), 7.019 (m, 6 H), 2.603 (s, 3 H), 2.098 (s, 6 H), −5.114 (t, J_{P-H} = 18.9 Hz, 1 H); mass spectrum (40 eV), m/e 835/833 (M^+), 572/570 (M^+ − PPh_3). Anal. Calcd for $ReP_2N_3C_{42}H_{40}$: C, 60.36; H, 4.79; N, 5.03. Found: C, 60.6; H, 4.9; N, 5.1.

$HRe(PPh_3)_2(CNC_2H_5)_3$. Complex **1** (75 mg, 0.096 mmol) and CNC_2H_5 (53 mg, 0.96 mmol) were sealed in a glass tube with C_6H_6 (1 mL) and heated to 50 °C for 3 h. Large yellow crystals (78 mg, 93%) were collected, washed with hexanes, and dried under vacuum: ^1H NMR (C_6D_6) δ 8.087 (m, 12 H), 7.161 (m, 12 H), 7.030 (t, J_{H-H} = 7.2 Hz, 6 H), 3.002 (q, J_{H-H} = 7.3 Hz, 2 H), 2.552 (q, J_{H-H} = 7.3 Hz, 4 H), 0.733 (t, J_{H-H} = 7.3 Hz, 3 H), 0.398 (t, J_{H-H} = 7.3 Hz, 6 H), −5.071 (t, J_{P-H} = 19.6 Hz, 1 H). Anal. Calcd for $ReP_2N_3C_{45}H_{46}$: C, 61.57; H, 5.25; N, 4.79. Found: C, 61.4; H, 5.3; N, 4.8.

$HRe(PPh_3)_2[CN(2\text{-}C_3H_7)]_3$. Complex **1** (75 mg, 0.096 mmol) was sealed in a glass tube with $CNCHMe_2$ (66 mg, 0.96 mmol) and C_6H_6 (1 mL) and heated to 50 °C for 3 h. The yellow microcrystalline product (80 mg, 90%) was washed with hexanes and dried under vacuum: ^1H NMR (C_6D_6) δ 8.083 (m, 12 H), 7.179

(18) *Organic Syntheses*: Wiley: New York, 1973; Coll. Vol. 5, pp 1060–1063.

(m, 12 H), 7.045 (t, J_{H-H} = 7.3 Hz, 6 H), 3.460 (septet, J_{H-H} = 6.2 Hz, 1 H), 3.039 (septet, J_{H-H} = 6.2 Hz, 2 H), 0.812 (d, J_{H-H} = 6.2 Hz, 6 H), 0.518 (d, J_{H-H} = 5.8 Hz, 12 H), −5.046 (t, J_{P-H} = 18.9 Hz, 1 H). Anal. Calcd for $ReP_2N_3C_{48}H_{52}$: C, 62.67; H, 5.66; N, 4.57. Found: C, 62.66; H, 5.66; N, 4.56.

$HRe(PPh_3)_2(CNCMe_3)_3$. Complex 1 (220 mg, 0.282 mmol) and $CNCMe_3$ (200 mg, 2.40 mmol) were sealed in a glass tube with C_6H_6 (2 mL) and heated to 50 °C for 2 h. Solvent was filtered away from the yellow crystalline material (219 mg, 81%). The product was washed with hexanes and dried under vacuum: ^1H NMR (C_6D_6) δ 8.065 (m, 12 H), 7.195 (m, 12 H), 7.048 (m, 6 H), 0.954 (s, 9 H), 0.711 (s, 18 H), −5.089 (t, J_{P-H} = 17.4 Hz, 1 H). Anal. Calcd for $ReP_2N_3C_{51}H_{58}$: C, 63.68; H, 6.03; N, 4.37. Found: C, 63.7; H, 6.0; N, 4.3.

$HRe(PPh_3)_2(CNCH_2CMe_3)_3$. Complex 1 (100 mg, 0.128 mmol) and $CNCH_2CMe_3$ (90 mg, 0.93 mmol) were sealed in a glass tube with C_6H_6 (2 mL) solvent and heated to 40 °C for 2 days. Solvent was removed with reduced pressure. The residue was dissolved in C_6H_6, and the yellow product was precipitated with hexanes (119 mg, 93%): ^1H NMR (C_6D_6) δ 8.091 (m, 12 H), 7.185 (m, 12 H), 7.059 (m, 6 H), 2.864 (s, 2 H), 2.506 (s, 4 H), 0.743 (s, 9 H), 0.486 (s, 18 H), −5.012 (t, J_{P-H} = 18.9 Hz, 1 H); $^{13}C\{^1H\}$ NMR (C_6D_6) δ 8.44 (d, J = 13 Hz), 18.81 (s), 19.09 (s), 24.09 (s), 47.85 (s), 48.21 (s), 127.03 (t, J = 5 Hz), 127.56 (s), 127.88 (s), 128.20 (s). Anal. Calcd for $ReP_2N_3C_{54}H_{64}$: C, 64.67; H, 6.39; N, 4.19. Found: C, 64.7; H, 6.6; N, 4.0.

$HRe(PPh_3)_2[CN(c\text{-}C_6H_{11})]_3$. Complex 1 (75 mg, 0.096 mmol) was sealed in a glass tube with $CN(c\text{-}C_6H_{11})$ (100 mg, 0.94 mmol) and C_6H_6 (1 mL) and heated to 50 °C for 6 h. Solvent and excess $CN(c\text{-}C_6H_{11})$ were removed with reduced pressure. The residue was dissolved in C_6H_6, and yellow microcrystalline product (64 mg, 64%) was precipitated with hexanes: ^1H NMR (C_6D_6) δ 8.109 (m, 12 H), 7.179 (m, 12 H), 7.052 (t, J_{H-H} = 7.2 Hz, 6 H), 3.293 (br s, 1 H), 2.926 (br s, 2 H), 1.25 (m, 3 H), −5.024 (t, J_{P-H} = 18.9 Hz, 1 H). Anal. Calcd for $ReP_2N_3C_{57}H_{64}$: C, 65.90; H, 6.17; N, 4.05. Found: C, 65.8; H, 6.1; N, 4.2.

$HRe(PPh_3)_2[CN(2,6\text{-}xyl)]_3$. Complex 1 (200 mg, 0.257 mmol) and CN(2,6-xyl) (xyl = xylyl) (269 mg, 2.1 mmol) were sealed in a glass tube with C_6H_6 (2 mL) and heated to 40 °C for 2 days. Solvent and excess CN(2,6-xyl) were removed with reduced pressure. The residue was dissolved in THF and precipitated with hexanes to produce a yellow crystalline solid (280 mg, 99%): ^1H NMR (C_6D_6) δ 8.051 (m, 12 H), 6.953 (m, 12 H), 6.650 (s, 6 H), 6.835 (m, 9 H), 2.236 (s, 6 H), 1.986 (s, 12 H), −4.021 (t, J_{P-H} = 20.4 Hz, 1 H). Anal. Calcd for $ReP_2N_3C_{63}H_{58}$: C, 68.52; H, 5.29; N, 3.80; P, 5.61. Found: C, 68.4; H, 5.3; N, 3.7; P. 5.5.

$HRe(PPh_3)_2(CO)_3$. Complex 1 (200 mg, 0.257 mmol) was dissolved in toluene (3 mL) and placed in a high-pressure stainless-steel bomb reactor under 350 psi of CO. After 8 h at 40 °C, the bomb reactor was opened and the solvent removed, yielding a white microcrystalline product (202 mg, 99%): ^1H NMR (C_6D_6) δ 7.822 (m, 12 H), 7.114 (m, 12 H), 7.016 (m, 6 H), −4.457 (t, J_{P-H} = 18.2 Hz, 1 H). Anal. Calcd for $ReP_2O_3C_{39}H_{31}$: C, 58.86; H, 3.93. Found: C, 58.64; H, 3.93.

Kinetics of the Reaction of 2,6-Xylyl Isocyanide with 1. The samples were prepared by dissolving 5 mg (6.42 mmol) of 1 in 2 mL of C_6D_6 and placing 0.6 mL of this solution in each of three NMR tubes attached to a ground glass joint. The appropriate amount of 2,6-xylyl isocyanide to give the concentrations indicated in Figure 2 was added to each sample, and the tubes were sealed under vacuum on the vacuum line. The tubes were heated in an oil bath and periodically examined by ^1H NMR spectroscopy. The areas of the free and coordinated xylyl resonances were used to determine the extent of reaction. For each sample, a plot of ln (% reaction) vs. time was linear for 1–3 half-lives.

Preparation of $HRe(PMe_3)_5$. Complex 1 (300 mg, 0.385 mmol) was placed in a glass tube with PMe_3 (300 mg, 3.90 mmol) and C_6H_6 (2 mL). The glass tube was sealed and heated to 40 °C for 2 days. Excess PMe_3 and solvent were removed with reduced pressure, and the residue was dissolved in ether and filtered. Slow evaporation of solvent produced large plate crystals: ^1H NMR (C_6D_6) δ 1.550 (br s, 36 H), 1.443 (d, J_{P-H} = 4.5 Hz, 9 H), −8.772 (quint of d, J_{Pa-H} = 23.2 Hz, J_{Pe-H} = 13.0 Hz, 1 H); $^{31}P\{^1H\}$ NMR (C_6D_6) δ −41.19 (d, J = 10 Hz, 4 P), −49.06 (quint, J = 10 Hz, 1 P); mass spectrum (70 eV), m/e 568/566 (M^+), 490/488 ($M^+ - PMe_3 - H_2$), 412/410 ($M^+ - 2PMe_3 - 2H_2$). Anal. Calcd for $ReP_5C_{15}H_{46}$: C, 31.74; H, 8.17. Found: C, 32.32; H, 8.54.

Preparation of $H_2Re(PEt_3)_3(PPh_2C_6H_4)$. Complex 1 (200 mg, 0.257 mmol) was placed in a glass tube with PEt_3 (300 mg, 2.54 mmol) and C_6H_6 (2 mL). The glass tube was sealed and heated to 45 °C for 18 h. Excess PEt_3 and solvent were removed with reduced pressure. Analytically pure crystals of $H_2Re(PEt_3)_3(PPh_2C_6H_4)$ were isolated upon addition of hexanes to the residue (191 mg, 93%). Slow evaporation of a saturated hexane solution yielded crystals suitable for X-ray study: ^1H NMR (toluene-d_8, −10 °C) δ 8.003 (m, 4 H), 7.716 (br s, 1 H), 7.008 (m, 9 H), 1.502 (br s, 6 H), 1.306 (br s, 12 H), 1.020 (br s, 9 H), 0.823 (br s, 18 H), −4.566 (br s, 1 H), −8.340 (br s, 1 H). Anal. Calcd for $ReP_4C_{36}H_{61}$: C, 53.78; H, 7.65. Found: C, 53.45; H, 7.67.

Preparation of Samples for Thermolysis and Photolysis of $HRe(PMe_3)_5$ Containing PMe_3 or $P(CD_3)_3$ in C_6D_6. For each sample complex **2h** (3 mg, 0.0053 mmol) was placed in an NMR tube under vacuum. PMe_3 (10 equiv) and C_6D_6 (0.4 mL) were condensed into the tube, and it was sealed. A similar sample was prepared by using $P(CD_3)_3$, and another sample with no phosphine. Mass spectra (70 eV) showed a distribution of isotopically substituted molecules centered around m/e 576.

Preparation of Samples Containing $HRe(PMe_3)_5$ with C_3H_8 in C_6D_6. Complex **2h** (3 mg, 0.0053 mmol) was placed in an NMR tube under vacuum. C_6D_6 (0.30 mL) and C_3H_8 (0.1 mL) were vacuum transferred into the tube, and it was sealed. No evidence for an H/D exchange between alkane and arene was observed upon photolysis or heating to 105 °C by ^2H NMR.

Preparation of Samples for Thermolysis and Photolysis of $HRe(PMe_3)_5$ in THF-d_8. Complex **2h** (3 mg, 0.0053 mmol) was placed in an NMR tube under vacuum. THF-d_8 (0.4 mL) was vacuum transferred into the tube, and it was sealed. No evidence for an H/D exchange between THF and hydride or coordinated PMe_3 was observed upon photolysis or heating to 105 °C by ^2H NMR. Photolysis was through a Pyrex Dewar maintained at −50 to −60 °C by periodic addition of LN_2 to a solution of CH_3OH/H_2O (55:45, v/v). The tube was maintained at −78 °C upon removal from the photolysis Dewar until it was dropped into the −70 °C NMR probe. A ^1H NMR spectrum showed the formation of free PMe_3 and several new hydride-containing products (see text) assigned as $HRe(PMe_3)_{5-x}(THF\text{-}d_8)_x$ (x = 1–3).

Reaction of $H_2Re(PEt_3)_3(PPh_2C_6H_4)$ with H_2. $H_2Re(PEt_3)_3(PPh_2C_6H_4)$ (2 mg, 0.0025 mmol) was placed under vacuum in an NMR tube. C_6D_6 (0.4 mL) was vacuum transferred into the tube, and an atmosphere of H_2 (700 Torr) was placed in the tube before it was sealed.

Reaction of $H_2Re(PEt_3)_3(PPh_2C_6H_4)$ with PEt_3. $H_2Re(PEt_3)_3(PPh_2C_6H_4)$ (2 mg, 0.0025 mmol) was placed under vacuum in an NMR tube. C_6D_6 (0.4 mL) was vacuum transferred into the tube followed by PEt_3 (7 equiv), and the tube was sealed.

Reaction of $H_2Re(PEt_3)_3(PPh_2C_6H_4)$ with PMe_3. $H_2Re(PEt_3)_3(PPh_2C_6H_4)$ (2 mg, 0.0025 mmol) was placed under vacuum in each NMR tube. C_6D_6 (0.4 mL) was vacuum transferred into each tube followed by PMe_3 (7 equiv), and each tube was sealed. One tube was heated in an oil bath to 105 °C, and irradiation of the second tube was through a 328-nm band-pass filter.

Reaction of $(\eta^4\text{-}C_5H_6)ReH_3(PPh_3)_2$ with DMPE. $(\eta^4\text{-}C_5H_6)ReH_3(PPh_3)_2$ (30 mg, 0.039 mmol) was placed in an NMR tube with DMPE (5 equiv) in the glovebox, and three freeze–pump–thaw degassing cycles were carried out. C_6D_6 (0.4 mL) and C_6H_6 (0.4 mL) were vacuum transferred into the tube, and it was sealed. The tube was heated to 50 °C in an oil bath for 2 weeks. ^1H NMR (27 °C) analysis indicated a mixture of isomers was present in solution (^1H NMR resonances observed for these complexes (THF-d_8): δ 7.430 (t, J = 8.0 Hz, 6 H), 7.034 (m, 9 H), 1.535 (s, 12 H), 1.125 (s, 12 H), and −10.878 (quint of d, J = 24.7 Hz, 16.0, 1 H) for $HRe(PPh_3)(DMPE)_2$ (PPh_3 trans to H) and δ 7.607 (t, J = 7.4 Hz, 6 H), 7.096 (m, 9 H), 1.777 (d, J = 7.7 Hz, 3 H), 1.480 (d, J = 5.0 Hz, 3 H), 1.433 (d, J = 5.4 Hz, 3 H), 1.307 (d, J = 5.5 Hz, 3 H), 1.255 (d, J = 4.9 Hz, 3 H), 1.171 (d, J = 5.2 Hz, 3 H), 0.544 (d, J = 4.8 Hz, 3 H), 0.266 (d, J = 5.8 Hz, 3 H),

Table IX. Summary of Crystallographic Data

	$HRe(PPh_3)_2(CNMe)_3$	$HRe(PMe_3)_5$	$H_2Re(PEt_3)_3(PPh_2C_6H_4)$	$HRe(PPh_3)(DMPE)_2 \cdot {}^1/_2C_6H_6$
		Crystal Parameters		
formula	$ReP_2N_3C_{42}H_{40}$	$ReP_5C_{15}H_{46}$	$ReP_4C_{36}H_{61}$	$ReP_5C_{33}H_{51}$
fw	834.96	567.60	819.10	788.84
cryst system	triclinic	monoclinic	orthorhombic	triclinic
space group	$P\bar{1}$	$C2/m$	$Pcab$	$P\bar{1}$
Z	2	4	8	2
a, Å	11.201 (5)	15.698 (6)	19.285 (5)	10.523 (6)
b, Å	18.630 (6)	10.869 (5)	32.437 (7)	18.599 (8)
c, Å	9.433 (4)	15.092 (4)	12.150 (4)	10.511 (5)
α, deg	98.74 (4)	90	90	90.94 (4)
β, deg	105.00 (4)	107.88 (3)	90	117.37 (4)
γ, deg	103.05 (4)	90	90	105.85 (5)
V, Å^3	1805.4 (3.3)	2450.5 (3.1)	7600.7 (5.7)	1732.9 (8.5)
d_{calcd}, g/cm^3	1.536	1.538	1.405	1.512
Xtal dimens, mm	0.34 × 0.19 × 0.15	0.56 × 0.52 × 0.23	0.34 × 0.26 × 0.22	0.12 × 0.23 × 0.34
temp, °C	25	−40	25	25
		Measurement of Intensity Data		
diffractometer		Enraf-Nonius CAD4, κ geometry		
radiatn (monochromator)		Mo, 0.71073 Å (graphite)		
scan type		$2\theta/\omega$		
scan rate, deg/min		2–16.5		
total bkgd time		scan time/2		
takeoff angle, deg		2.6		
scan range, deg	0.7 + 0.35 tan θ	0.7 + 0.35 tan θ	0.6 + 0.35 tan θ	0.6 + 0.35 tan θ
2θ range, deg	4–44	4–40	4–40	4–44
data collected	$+h,\pm k,\pm l$	$+h,+k,\pm l$	$+h,+k,+l$	$+h,\pm k,\pm l$
no. of data collected	4740	1281	4141	4506
no. of unique data > 3σ	3820	1212	2089	3899
no. of parameters varied	433	107	376	356
abs coeff, cm^{-1}	35.30	53.45	34.29	38.01
systematic absences	none	hkl, $h + k$ odd	$0kl$, l odd; $h0l$, h odd; $hk0$, k odd	none
abs correctn	empirical	empirical	empirical	empirical
range of transmissn factors	47.8–99.9	40.2–99.9	67.7–100.0	57.0–99.9
equiv data	$0kl = 0k\bar{l}$	$0kl = 0k\bar{l}$	$hkl = hk\bar{l}$	$0kl = 0k\bar{l}$
agreement between equiv/data (F_o)	0.026	0.009	0.026	0.01
R_1	0.060	0.025	0.027	0.017
R_2	0.073	0.044	0.036	0.024
goodness of fit	2.33	1.45	1.33	1.00

and −8.381 (m, 1 H) for $HRe(PPh_3)(DMPE)_2$ (PPh_3 cis to H)). Upon standing and as slow evaporation of C_6D_6 continued, orange crystals precipitated. The ^1H NMR of these crystals is consistent with the single isomer of $HRe(DMPE)_2(PPh_3)$ with PPh_3 cis to hydride. Recrystallization from THF/hexane gave analytically pure product. Anal. Calcd for $ReP_5C_{30}H_{48}$: C, 48.06; H, 6.45. Found: C, 48.62; H, 6.32.

Isomerization of *cis*-$HRe(DMPE)_2(PPh_3)$ to *trans*-$HRe(DMPE)_2(PPh_3)$ in THF-d_8. *cis*-$HRe(DMPE)_2(PPh_3)$ (2 mg, 0.0027 mmol) was placed in an NMR tube under N_2. The isomerization of *cis*-$HRe(DMPE)_2(PPh_3)$ to *trans*-$HRe(DMPE)_2(PPh_3)$ was observed to go to a 1:1.44 ratio by integration of the distinct ortho phenyl resonances via ^1H NMR at 27 °C.

Variable-Temperature Equilibrium Ratios of the Two $HRe(DMPE)_2(PPh_3)$ Isomers. $HRe(DMPE)_2(PPh_3)$ (2 mg, 0.0027 mmol) was placed in an NMR tube in the glovebox where THF-d_8 (0.2 mL) and C_6D_6 (0.2 mL) were added. Integration of the areas of the well-separated ortho phenyl proton resonances of each isomer were used to measure the equilibrium concentrations for the isomers at various temperatures using ^1H NMR from −10 to 58 °C. These ratios varied from 1.67:1 at −10 °C to 1.41:1 at 58 °C for the trans to cis isomers, respectively.

Isomerization of *cis*-$HRe(DMPE)_2(PPh_3)$ in the Presence of PPh_3-d_{15}. *cis*-$HRe(DMPE)_2(PPh_3)$ (2 mg, 0.0027 mmol) and PPh_3-d_{15} (2 mg, 6 equiv) were placed in an NMR tube with THF-d_8 (0.4 mL), and the tube was sealed with a septum and parafilm. ^1H NMR spectroscopy was used to follow the isomerization progress. Only resonances for the two isomers of $HRe(DMPE)_2(PPh_3)$ were observed, and no resonance was observed for uncoordinated PPh_3.

General Procedure for Structural Determinations. Following mounting of the crystal with epoxy on a glass fiber, lattice constants were obtained from 25 centered reflections with values of χ between 0° and 60°. Cell reduction with the program TRACER revealed the crystal system. Data were collected on the crystal in accord with the parameters in Table IX. Patterson map determination of the rhenium position allowed solution of the structure, and subsequent difference Fourier and full-matrix least-squares refinement converged to the final solution. The Molecular Structure Corp. SDP package was used for solution and refinement of the structure.[19]

X-ray Structural Determination of $HRe(PPh_3)_2(CNMe)_3$. Well-formed crystals of the complex were grown by slow evaporation of a saturated benzene solution of **2a** in an N_2 inert atmosphere, washed with hexane, and dried under vacuum. The triclinic space group was assigned as $P\bar{1}$ ($P1$ also possible), and the correctness of this centric choice was confirmed by successful solution of the structure. Phenyl hydrogen atoms were placed in idealized positions with the program HYDRO, and no attempt was made to place the nine methyl hydrogens. A final difference Fourier map and peak search failed to show any peaks near the metal in proper position to be the hydride ligand. Final anisotropic refinement of all non-hydrogen atoms was carried out with fixed positional and thermal (B = 5.0 Å^2) parameters for the 30 phenyl hydrogen atoms. Table I contains the relevent bond distances and angles, and Table II includes the positional parameters.

X-ray Structural Determination of $HRe(PMe_3)_5$. Large well-formed plate crystals were grown by slow evaporation of a saturated ether solution. The monoclinic space group was assigned as $C2/m$, and the correctness of this choice was confirmed by successful solution of the Patterson map. Methyl group hydrogens

(19) $R_1 = \{\sum||F_o| - |F_c||\}/\{\sum|F_o|\}$ and $R_2 = \{\sum w(|F_o| - |F_c|)^2\}^{1/2}/\{\sum wF_o^2|\}$, where $w = \{\sigma^2(F_o) + [pF_o^2]^2\}^{1/2}$ for the non-Poisson contribution weighting scheme. The quantity minimized was $\sum w\cdot(|F_o| - |F_c|)^2$. Source of scattering factors f_o, f', and f'': Cromer, D. T.; Waber, J. T. *International Tables for X-Ray Crystallography*; Kynoch: Birmingham, England, 1974; Vol. IV, Tables 2.2B and 2.3.1.

were placed in idealized staggered tetrahedral positions by using the program HYDRO. Final refinement of the positions of all non-hydrogen atoms was carried out anisotropically with fixed hydrogen positions and thermal parameters (B = 5.0 Å^2). A final difference Fourier map showed a peak (1.2 e/Å^3) located near the octahedral hole where the hydride was expected to be located, but not in an ideal location. Table III contains the relevent bond distances and angles, and Table IV includes the positional parameters.

X-ray Structural Determination of $H_2\overline{Re(PEt_3)_3(PPh_2C_6H_4)}$. Slow evaporation of a saturated benzene solution yielded large crystals. The orthorhombic space group was assigned as *Pcab*, and the correctness of this assignment was confirmed by successful solution of the Patterson map. Hydrogen atoms were placed in idealized positions on carbon atoms by using the program HYDRO. After a final anisotropic least-squares refinement of all non-hydrogen atoms, a final peak search revealed only two large peaks in the map near the rhenium atom in the equatorial plane in locations expected for the two hydride ligands. These atoms were placed in the structure, and their positions were refined while the thermal parameters were fixed (B = 5.0 Å^2). Table V contains the relevent bond distances and angles, and Table VI includes the positional parameters.

X-ray Structural Determination of $HRe(PPh_3)(DMPE)_2$. Slow evaporation of a saturated benzene solution yielded large crystals. The triclinic space group $P\bar{1}$ was assigned, and the correctness of this assignment was confirmed by successful solution of the Patterson map. A benzene of crystallization was located on a center of symmetry. Hydrogen atoms were placed in idealized positions on carbon atoms by using the program HYDRO. After a final anisotropic least-squares refinement of all non-hydrogen atoms a final peak search revealed only a large peak in the map near the rhenium atom in the octahedral hole. Final refinement was carried out anisotropically on all non-hydrogen atoms and isotropically on the hydride. Table VII contains the relevent bond distances and angles, and Table VIII includes the positional parameters.

Acknowledgment is made to the U.S. Department of Energy (DE-FG02-86ER13569) for their partial support of this work. W.D.J. also thanks the Alfred P. Sloan and Camille and Henry Dreyfus Foundations for awards. We also thank Mr. M. Fan for his assistance in obtaining spectral data.

Registry No. **1**, 81368-84-5; **2a**, 108453-34-5; **2b**, 108453-35-6; **2c**, 108453-36-7; **2d**, 108453-37-8; **2e**, 108453-38-9; **2f**, 108453-39-0; **2g**, 108453-40-3; **2h**, 84756-10-5; $HRe(PPh_3)^2(CO)_3$, 25734-54-7; $H_2\overline{Re(PEt_3)_3(PPh_2C_6H_4)}$, 108453-41-4; *trans*-$HRe(PPh_3)(DMPE)_2$, 108453-42-5; *cis*-$HRe(DMPE)_2(PPh_3{\cdot}^1/_2C_6H_6$, 108509-40-6.

Supplementary Material Available: Listings of anisotropic thermal parameters, bond distances and angles, calculated fractional coordinates for $HRe(PMe_3)_5$, $HRe(PPh_3)_2(CNMe)_3$, $H_2\overline{Re(PEt_3)_3(PPh_2C_6H_4)}$, and $HRe(PPh_3)(DMPE)_2$ (43 pages); listings of calculated and observed structure factors (112 pages). Ordering information is given on any current masthead page.

Bridged Ferrocenes. 13.[1] Preparation and Properties of Derivatives with β-Oxatrimethylene Bridges

Manny Hillman* and Joyce D. Austin

Chemical Sciences Division, Department of Applied Science, Brookhaven National Laboratory, Upton, New York 11973

Received October 28, 1986

Ferrocene derivatives containing one β-oxatrimethylene and 0–2 trimethylene bridges were prepared. The X-ray crystallographic structures of all but the one containing two trimethylene bridges were determined. The X-ray crystallographic structures of 1,1′-trimethyleneferrocene (I), 1,1′-(β-thiatrimethylene)ferrocene (III), and the two bis(trimethylene)ferrocenes IV and VI were also determined. The reduction potentials of all of the (β-oxatrimethylene)ferrocenes and the (β-thiatrimethylene)ferrocene were newly measured and compared with the reduction potentials of the corresponding trimethyleneferrocenes that were remeasured. Evidence was found for an interaction between the iron atom and the oxygen atom of the bridge that is comparable to that suggested previously for the central methylene group of a trimethylene bridge, but not significantly greater.

Introduction

Simple alkyl substituents and homoannular trimethylene groups all cause the ferrocene derivative to be more easily oxidized by the same amount for each substituent (counting the homoannular trimethylene group as two substituents). On the other hand, a bridging trimethylene group makes the derivative more easily oxidized by a substantially smaller amount. Furthermore, the influence of the trimethylene bridge can be correlated with the iron-to-ring distance of each compound. Since the electron distribution around the iron atom is oblate and the oblateness increases with a decreased iron-to-ring distance, the effect of bridges on the reduction potentials was attributed[2] to an increased interaction of the iron atom with the central methylene of the bridge as the iron-to-ring distance decreases.

To test this hypothesis, we undertook the investigation of the properties of ferrocene derivatives containing central groups on the bridges that are expected to be more interactive with the iron atom than are methylene groups. The primary candidates for this investigation were the (β-oxotrimethylene)ferrocenes wherein the carbonyl group would most certainly be expected to be more interactive than the methylene. Spatial models indicate that the

(1) Paper 12 of series: Hillman, M.; Austin, J. D. *Organometallics* **1985**, *3*, 316–320.

(2) Fujita, E.; Gordon, B.; Hillman, M.; Nagy, A. *J. Organomet. Chem.* **1981**, *218*, 105–114.

0276-7333/87/2306-1737$01.50/0